

Quantum dynamics within curved thin layers with deviation

Run Cheng(程润), Hao Zhao(赵浩), Cui-Bai Luo(罗翠柏), Xuan Zhou(周璇), Bi-Li Wang(王必利), Yan-Biao Li(李延标), and Jun Wang(王骏)

Citation: Chin. Phys. B, 2024, 33 (**7**): 076801. DOI: 10.1088/1674-1056/ad3dd2
Journal homepage: http://cpb.iphy.ac.cn; http://iopscience.iop.org/cpb

What follows is a list of articles you may be interested in

Molecular beam epitaxy growth of quantum devices

Ke He(何珂)
Chin. Phys. B, 2022, 31 (**12**): 126804. DOI: 10.1088/1674-1056/aca6d3

In-plane optical anisotropy of two-dimensional VOCl single crystal with weak interlayer interaction

Ruijie Wang(王瑞洁), Qilong Cui(崔其龙), Wen Zhu(朱文), Yijie Niu(牛艺杰), Zhanfeng Liu(刘站锋), Lei Zhang(张雷), Xiaojun Wu(武晓君), Shuangming Chen(陈双明), and Li Song(宋礼)
Chin. Phys. B, 2022, 31 (**9**): 096802. DOI: 10.1088/1674-1056/ac7555

Surface electron doping induced double gap opening in T_d-WTe_2

Qi-Yuan Li(李启远), Yang-Yang Lv(吕洋洋), Yong-Jie Xu(徐永杰), Li Zhu(朱立), Wei-Min Zhao(赵伟民), Yanbin Chen(陈延彬), and Shao-Chun Li(李绍春)
Chin. Phys. B, 2022, 31 (**6**): 066802. DOI: 10.1088/1674-1056/ac632e

C_9N_4 as excellent dual electrocatalyst: A first principles study

Wei Xu(许伟), WenWu Xu(许文武), and Xiangmei Duan(段香梅)
Chin. Phys. B, 2021, 30 (**9**): 096802. DOI: 10.1088/1674-1056/ac0ccf

Strain-tunable electronic and optical properties of h-BN/BC_3 heterostructure with enhanced electron mobility

Zhao-Yong Jiao(焦照勇), Yi-Ran Wang(王怡然), Yong-Liang Guo(郭永亮), and Shu-Hong Ma(马淑红)
Chin. Phys. B, 2021, 30 (**7**): 076801. DOI: 10.1088/1674-1056/abe29d

---

Quantum dynamics within curved thin layers with deviation

Run Cheng(程润)[1,†], Hao Zhao(赵浩)[3], Cui-Bai Luo(罗翠柏)[4], Xuan Zhou(周璇)[1], Bi-Li Wang(王必利)[1], Yan-Biao Li(李延标)[1,‡], and Jun Wang(王骏)[2,§]

[1] *Physics Department of Basic Department, Army Engineering University of PLA, Nanjing* 211101, *China*
[2] *National Laboratory of Solid State Microstructure, Collaborative Innovation Center of Advanced Microstructures, and School of Physics, Nanjing University, Nanjing* 210093, *China*
[3] *School of Physics and Electronics, Hunan University, Changsha* 410082, *China*
[4] *Department of Physics, Anhui Normal University, Wuhu* 241002, *China*

(Received 23 February 2024; revised manuscript received 10 April 2024; accepted manuscript online 12 April 2024)

Combining the deviation between thin layers' adjacent surfaces with the confining potential method applied to the quantum curved systems, we derive the effective Schrödinger equation describing the particle constrained within a curved layer, accompanied by a general geometric potential $V_{\rm gq}$ composed of a compression-corrected geometric potential $V_{\rm gq}^{*}$ and a novel potential $V_{\rm gq}^{**}$ brought by the deviation. Applying this analysis to the cylindrical layer emerges two types of deviation-induced geometric potential, resulting from the the cases of slant deviation and tangent deviation, respectively, which strongly renormalizes the purely geometric potential and contribute to the energy spectrum based on a very substantial deepening of bound states they offer.

Keywords: confining potential method, quantum mechanics, curved thin layer

PACS: 68.65.–k, 03.65.–w, 02.40.–k **DOI:** 10.1088/1674-1056/ad3dd2

1. Introduction

Quantum dynamics on curved surface has engaged much attention of physicists, accompanied by the advanced developments of nano-technology and low-dimensional materials.[1–4] As examples, subject to the relaxation of elastic stress of the thin solid film, the roll-up nanotubes and nano-corrugated structures has been successfully fabricated.[5,6] It has been observed that the spatial geometry produces systematic effects on the dynamics and spectrum of confined electron,[7–10] which not only demonstrate the importance of surface curvature, but also stimulate the need of the theory to study low-dimensional curved systems.

Physically, the confining potential method[11,12] has widely been applied in the studies of low-dimensional systems. As an important consequence, the geometric potential $V_{\rm g}$ taken as the equivalent of the geometric deformation appears in the effective Schrödinger equation, which depends not only on the intrinsic curvature provided by the surface geometry, but also on the extrinsic curvature results from the exterior normal of the embedded surface.[11–15] Specifically, the existence of $V_{\rm g}$ results in the appearance of atomic-like bound states on the two-dimensional sheet rolled up into an Archimedean spiral,[5] and reconstructs electron level structures on corrugated nanotubes.[7,8] Moreover, the relativity-corrected geometric potential in Minkowski space[16,17] and the spin connection geometric potential acting on spin particles[17,18] are obtained, which contributes to modulating the transport properties and spin-flip behavior of the particle. Importantly, the validity of this method was further verified by optical analogue realizations of the geometric potential in photonic crystal.[19]

Methodically, researchers normally treat the curved thin layer as a surface in previous applications, where the introduced compression direction is along the surface normal.[11,12] While during the process of synthesizing nano-materials, the incompatibilities between the substrate and the attachment are sometimes brought,[2,4,20–22] which leads to the deviation between adjacent surfaces of the thin layers. However, there are no theories to consider both the curvature and surfaces' deviation of the layer. How do these two effects interplay with each other and modulate the quantum behaviors of particles within curved thin layers? Our work is an approach towards such a problem theoretically.

In our work, we focus on the quantum dynamics of the particle within curved layers. The confining potential method is carried out to constrain the particle, where the deviation is incorporated to characterize the change of the compression direction. To explicitly exemplify the contribution of geometric effects in this case, an effective Schrödinger equation for the curved thin layers with deviations is proposed. In this equation, the well-known geometric potential still exists and is deformed by the compression direction, but also a novel effective potential related to the adjacent surfaces' deviations is observed. With these effective potentials, the contributions of the deviation on the energy spectrum are discussed. These establish a procedure to analyze the quantum behaviors

†Corresponding author. E-mail: chengrphy@126.com
‡Corresponding author. E-mail: liyanbiao@yeah.net
§Corresponding author. E-mail: wangj@nju.edu.cn

© 2024 Chinese Physical Society and IOP Publishing Ltd

within curved thin layers and generalize the confining potential method.

The outline for our paper is given as follows. In Section 2, we derive the effective Schrödinger equation describing the particle constrained within the curved layer. In Section 3, based on the surface Schrödinger equation, the behaviors of the particle on cylindrical geometries are specifically analyzed, focusing on the effect of two specific types of the deviations. Finally, we draw our conclusion and discussion in Section 4.

2. Schrödinger equation within curved thin layers with deviations

To begin with, we consider a surface $S \subset R^3$ that is represented by a parameterization of $S = S(q^a, q^b)$, where q^a and q^b are the surface coordinate components. In this way, the thin layer with S as the base can be parameterized as

$$\begin{aligned} \boldsymbol{R}(q^a,q^b,q^3) &= \boldsymbol{r} + q^3\boldsymbol{n}'(q^a,q^b), \\ \boldsymbol{n}' &= \frac{\boldsymbol{n}+\delta\boldsymbol{r}}{[1+(\delta\boldsymbol{r})^2]^{1/2}}, \\ \delta\boldsymbol{r} &= \frac{\partial \boldsymbol{r}}{\partial q^a}\delta r_a + \frac{\partial \boldsymbol{r}}{\partial q^b}\delta r_b = \boldsymbol{r}'_a\delta r_a + \boldsymbol{r}'_b\delta r_b, \end{aligned} \tag{1}$$

where $\boldsymbol{r}$ denotes the position vector on S, q^3 is the curvilinear coordinate along $\boldsymbol{n}'$, as shown in Fig. 1. The general compression direction vector $\boldsymbol{n}'$ is thus composed of $\delta\boldsymbol{r}$ and $\boldsymbol{n}$, which are the disturbance along the tangential plane spanned by two tangent unit basis vector $\boldsymbol{e}_{q^a}, \boldsymbol{e}_{q^b}$ and the normal unit basis vector of S, respectively.

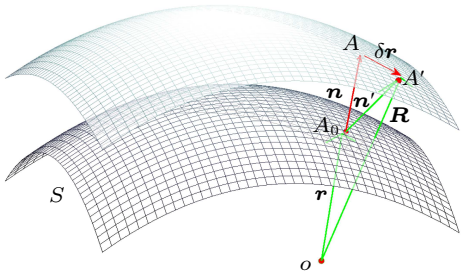


Fig. 1. The curved thin layer with the deviation.

Accordingly, for the coordinate system defined in Eq. (1), the metric tensor G_{ab} in the three-dimensional (3D) space can be expressed in terms of surface metrics[23] $g_{ab} = \partial_a\boldsymbol{r}\cdot\partial_b\boldsymbol{r}$ $(a,b=1,2)$ as

$$\begin{aligned} G_{ab} &= \frac{\partial R}{\partial q^a}\cdot\frac{\partial R}{\partial q^b} \\ &= \left(\frac{\partial \boldsymbol{r}}{\partial q^a} + q^3\frac{\partial \boldsymbol{n}'}{\partial q^a}\right)\cdot\left(\frac{\partial \boldsymbol{r}}{\partial q^b} + q^3\frac{\partial \boldsymbol{n}'}{\partial q^b}\right) \\ &= g_{ab} - 2\alpha^{*c}_{\ a}q^3 g_{cb} + \alpha^{*c}_{\ a}\alpha^{*d}_{\ b}(q^3)^2 g_{cd}, \\ G_{a3} &= G_{3a} = \left(\frac{\partial \boldsymbol{r}}{\partial q^a} + q^3\frac{\partial \boldsymbol{n}'}{\partial q^a}\right)\cdot\boldsymbol{n}', \\ G_{33} &= 1, \end{aligned} \tag{2}$$

where $\alpha^{*b}_{\ a}$ is the corrected Weingarten curvature matrix[12] defined as

$$\frac{\partial \boldsymbol{n}'}{\partial q^a} = -\alpha^{*b}_{\ a}\frac{\partial \boldsymbol{r}}{\partial q^b}. \tag{3}$$

Taking $\delta\boldsymbol{r}'_a = \partial\delta\boldsymbol{r}/\partial q^a$, $\delta\boldsymbol{r}'_b = \partial\delta\boldsymbol{r}/\partial q^b$, $\boldsymbol{n}'_a = \partial\boldsymbol{n}/\partial q^a$, and $\boldsymbol{n}'_b = \partial\boldsymbol{n}/\partial q^b$ will yield

$$\begin{aligned} \begin{pmatrix} \alpha^{*a}_{\ a} & \alpha^{*a}_{\ b} \\ \alpha^{*b}_{\ a} & \alpha^{*b}_{\ b} \end{pmatrix} &= \frac{1}{[1+(\delta\boldsymbol{r})^2]^{1/2}}\frac{1}{|g|} \\ &\times \begin{pmatrix} L-\delta\boldsymbol{r}'_a\cdot\boldsymbol{r}'_a & M-\delta\boldsymbol{r}'_a\cdot\boldsymbol{r}'_b \\ M-\delta\boldsymbol{r}'_b\cdot\boldsymbol{r}'_a & N-\delta\boldsymbol{r}'_b\cdot\boldsymbol{r}'_b \end{pmatrix} \\ &\times \begin{pmatrix} G & -F \\ -F & E \end{pmatrix}, \end{aligned} \tag{4}$$

where $|g|$ is the determinant of g_{ab} and the parameters of the first and second fundamental forms of a surface are expressed as

$$\begin{aligned} E &= \boldsymbol{r}'_a\cdot\boldsymbol{r}'_a, \quad F = \boldsymbol{r}'_a\cdot\boldsymbol{r}'_b, \quad G = \boldsymbol{r}'_b\cdot\boldsymbol{r}'_b, \\ L &= -\boldsymbol{r}'_a\cdot\boldsymbol{n}'_a, \quad M = -\boldsymbol{r}'_a\cdot\boldsymbol{n}'_b = -\boldsymbol{r}'_b\cdot\boldsymbol{n}'_a, \\ N &= -\boldsymbol{r}'_b\cdot\boldsymbol{n}'_b, \end{aligned} \tag{5}$$

then the effective mean curvature H^* and Gaussian curvature K^* can be written as

$$\begin{aligned} H^* &= \frac{\alpha^{*a}_{\ a}+\alpha^{*b}_{\ b}}{2} = \frac{1}{[1+(\delta\boldsymbol{r})^2]^{1/2}}\left[H + \frac{-G\delta\boldsymbol{r}'_a\cdot\boldsymbol{r}'_a - E\delta\boldsymbol{r}'_b\cdot\boldsymbol{r}'_b + F(\delta\boldsymbol{r}'_a\cdot\boldsymbol{r}'_b + \delta\boldsymbol{r}'_b\cdot\boldsymbol{r}'_a)}{2|g|}\right], \\ K^* &= \det(\alpha^*) = \frac{1}{[1+(\delta\boldsymbol{r})^2]}\left[K + \frac{-N\delta\boldsymbol{r}'_a\cdot\boldsymbol{r}'_a - L\delta\boldsymbol{r}'_b\cdot\boldsymbol{r}'_b + M(\delta\boldsymbol{r}'_a\cdot\boldsymbol{r}'_b + \delta\boldsymbol{r}'_b\cdot\boldsymbol{r}'_a)}{|g|}\right], \end{aligned} \tag{6}$$

where H and K are the curvatures of S. According to the Eq. (2), $|G|$ known as the determinant of G_{ij} $(i,j=1,2,3)$ can be expressed as

$$|G| = G_{aa}G_{bb}(1-\cos^2\theta_{a3}-\cos^2\theta_{b3}) - G_{ab}G_{ba},$$

$$\begin{aligned} \cos\theta_{a3} &= \frac{1}{[1+(\delta\boldsymbol{r})^2]^{1/2}}\frac{\boldsymbol{r}'_a\cdot\delta\boldsymbol{r}}{|\boldsymbol{r}'_a+q^3\partial_a\boldsymbol{n}'|} \\ &= \frac{1}{[1+(\delta\boldsymbol{r})^2]^{1/2}}\frac{E\delta r_a + F\delta r_b}{|\boldsymbol{r}'_a+q^3\partial_a\boldsymbol{n}'|}, \\ \cos\theta_{b3} &= \frac{1}{[1+(\delta\boldsymbol{r})^2]^{1/2}}\frac{\boldsymbol{r}'_b\cdot\delta\boldsymbol{r}}{|\boldsymbol{r}'_b+q^3\partial_b\boldsymbol{n}'|} \end{aligned}$$

$$= \frac{1}{[1+(\delta\boldsymbol{r})^2]^{1/2}} \frac{F\delta r_a + G\delta r_b}{|\boldsymbol{r}'_b + q^3\partial_b\boldsymbol{n}'|}, \tag{7}$$

where $\partial_a\boldsymbol{n}' = \partial\boldsymbol{n}'/\partial q^a$ and $\partial_b\boldsymbol{n}' = \partial\boldsymbol{n}'/\partial q^b$. Generally, $\boldsymbol{e}_{q^a} \perp \boldsymbol{e}_{q^b}$, namely, the orthogonal coordinates leads to $F = M = 0$. Therefore, equation (6) can be rewritten as

$$\begin{aligned}
H^* &= \frac{1}{[1+(\delta\boldsymbol{r})^2]^{1/2}}\left[H + \frac{-G\delta\boldsymbol{r}'_a\cdot\boldsymbol{r}'_a - E\delta\boldsymbol{r}'_b\cdot\boldsymbol{r}'_b}{2|g|}\right],\\
K^* &= \frac{1}{[1+(\delta\boldsymbol{r})^2]}\left[K + \frac{-N\delta\boldsymbol{r}'_a\cdot\boldsymbol{r}'_a - L\delta\boldsymbol{r}'_b\cdot\boldsymbol{r}'_b}{|g|}\right],\\
\delta\boldsymbol{r}'_a &= \frac{\partial(\delta r_a)}{\partial q^a}\boldsymbol{r}'_a + \delta r_a\frac{\partial^2\boldsymbol{r}}{\partial(q^a)^2} + \frac{\partial(\delta r_b)}{\partial q^a}\boldsymbol{r}'_b + \delta r_b\frac{\partial^2\boldsymbol{r}}{\partial q^b q^a},\\
\delta\boldsymbol{r}'_b &= \frac{\partial(\delta r_a)}{\partial q^b}\boldsymbol{r}'_a + \delta r_a\frac{\partial^2\boldsymbol{r}}{\partial q^a q^b} + \frac{\partial(\delta r_b)}{\partial q^b}\boldsymbol{r}'_b + \delta r_b\frac{\partial^2\boldsymbol{r}}{\partial(q^b)^2}.
\end{aligned} \tag{8}$$

For simplicity, keeping the consistency of the compression direction around S determines that the $\delta\boldsymbol{r}$ is independent of (q^a, q^b). Consequently, equations (7) and (8) turn into

$$\begin{aligned}
\cos^2\theta_{a3} &= \frac{1}{[1+(\delta\boldsymbol{r})^2]}\frac{E^2{\delta r_a}^2}{E + (q^3)^2 + \frac{2q^3(-L)}{[1+(\delta\boldsymbol{r})^2]^{1/2}}},\\
\cos^2\theta_{b3} &= \frac{1}{[1+(\delta\boldsymbol{r})^2]}\frac{G^2{\delta r_b}^2}{G + (q^3)^2 + \frac{2q^3(-N)}{[1+(\delta\boldsymbol{r})^2]^{1/2}}},\\
H^* &= \frac{1}{[1+(\delta\boldsymbol{r})^2]^{1/2}}H, \quad K^* = \frac{1}{[1+(\delta\boldsymbol{r})^2]}K.
\end{aligned} \tag{9}$$

Combing Eqs. (2) and (9), $|G|$ and $|g|$ satisfy the relationship

$$\begin{aligned}
|G| &= (f + f_\delta)|g| = f^*|g|,\\
f &= [1 - 2H^*q^3 + K^*(q^3)^2]^2,\\
f_\delta &= -[1 - 2q^3\alpha'^a_a + (q^3)^2(\alpha'^a_a)^2]\\
&\quad\times[1 - 2q^3\alpha'^b_b + (q^3)^2(\alpha'^b_b)^2](\cos^2\theta_{a3} + \cos^2\theta_{b3})\\
&= -[1 - 2H^*q^3 + K^*(q^3)^2]^2(\cos^2\theta_{a3} + \cos^2\theta_{b3}),\\
f^* &= [1 - 2H^*q^3 + K^*(q^3)^2]^2(1 - \cos^2\theta_{a3} - \cos^2\theta_{b3}),
\end{aligned} \tag{10}$$

where f^* is the corrected rescaling factor.[7]

Following Refs. [11,12], we next investigate the behaviors of particles constrained within the curved layer based on the Schrödinger equation

$$\mathrm{i}\hbar\frac{\partial\psi}{\partial t} = -\frac{\hbar^2}{2m}\left(\frac{1}{\sqrt{G}}\frac{\partial}{\partial q^i}\sqrt{G}G^{ij}\frac{\partial\psi}{\partial q^j}\right) + V_\lambda\psi, \tag{11}$$

where $\hbar$ is the Planck constant divided by 2π, m is the mass of the particle, and the squeezing potential $V = V_\lambda(q^3)$ is introduced to keep the particles always attached to the predetermined surface. To investigate the geometric effect, we decouple the wave function $\psi(q^1, q^2, q^3, t)$ as

$$\begin{aligned}
\psi(q^1, q^2, q^3, t) &= \left(\frac{|G|}{|g|}\right)^{-1/4}\psi'(q^1, q^2, q^3, t)\\
&= f^{*-1/4}\chi_{\mathrm{s}}(q^1, q^2, t)\chi_{\mathrm{n}}(q^3, t)
\end{aligned} \tag{12}$$

based on the conservation of probability density

$$\int|\psi|^2\sqrt{G}\mathrm{d}q^1\mathrm{d}q^2\mathrm{d}q^3 = \int|\chi_{\mathrm{s}}|^2|\chi_{\mathrm{n}}|^2\sqrt{g}\mathrm{d}q^1\mathrm{d}q^2\mathrm{d}q^3, \tag{13}$$

where χ_{s} and χ_{n} are wave functions defined on the surface and along the normal direction, respectively. Under such a circumstance, by substituting Eq. (12) into Eq. (11), we separate Eq. (11) into a surface part and a normal part as follows:

$$\begin{aligned}
\mathrm{i}\hbar\frac{\partial\chi_{\mathrm{s}}}{\partial t} &= -\frac{\hbar^2}{2m}\frac{1}{\sqrt{g}}\partial_a\left[g^{ab}\sqrt{g}\frac{\partial\chi_{\mathrm{s}}}{\partial q^b}\right] + V_{\mathrm{gq}}\chi_{\mathrm{s}},\\
\mathrm{i}\hbar\frac{\partial\chi_{\mathrm{n}}}{\partial t} &= -\frac{\hbar^2}{2m}\frac{\partial^2\chi_{\mathrm{n}}}{\partial {q^3}^2} + V_\lambda\chi_{\mathrm{n}}.
\end{aligned} \tag{14}$$

The general geometric potential V_{gq} ($q^3 \to 0$) can be derived as

$$\begin{aligned}
C^* &= \frac{1}{1+\delta\boldsymbol{r}^2} = \frac{1}{1 + E{\delta r_a}^2 + G{\delta r_b}^2},\\
C^{**} &= \frac{-2(L{\delta r_a}^2 + N{\delta r_b}^2)}{(1+\delta\boldsymbol{r}^2)^{3/2}} = \frac{-2(L{\delta r_a}^2 + N{\delta r_b}^2)}{(1 + E{\delta r_a}^2 + G{\delta r_b}^2)^{3/2}},\\
V_{\mathrm{gq}} &= -\frac{\hbar^2}{2m}f^{*-1/4}\partial_3[f^{*1/4}\partial_3[\ln(f^{*-1/4})]]_{q^3\to 0}\\
&= V^*_{\mathrm{gq}} + V^{**}_{\mathrm{gq}},\\
V^*_{\mathrm{gq}} &= -\frac{\hbar^2}{2m}\left[C^*(H^2 - K) + \frac{H}{2}\frac{C^{**}}{\sqrt{C^*}}\right],\\
V^{**}_{\mathrm{gq}} &= -\frac{\hbar^2}{2m}\left[-\frac{({\delta r_a}^2 + {\delta r_b}^2)}{2}\right.\\
&\quad\left.+\frac{2C^*(GL^2{\delta r_a}^2 + EN^2{\delta r_b}^2)}{EG} + \frac{3C^{**2}}{16C^{*2}}\right].
\end{aligned} \tag{15}$$

It is worth noting that V_{gq} is composed of V^*_{gq} and V^{**}_{gq}, the former is the curvature-dependent term that consists of two parts. One is the deformed version of the well-known geometric potential $-\frac{\hbar^2}{2m}C^*(H^2 - K)$, where the first corrected factor C^* related to the length of the deviation $\delta\boldsymbol{r}$ that is written as the first fundamental form of S, the other part $-\frac{\hbar^2}{4m}\frac{HC^{**}}{\sqrt{C^*}}$ is the coupled term where the second corrected factor C^{**} related to the second fundamental form of S, representing the projection of the deviation in $\boldsymbol{n}$. The latter V^{**}_{gq} is the novel potential that is independent of curvatures, which is originated from the coupling between the surface metrics and the deviation.

And it is worth noting that when $|\delta\boldsymbol{r}| = 0$, the compression direction returns to $\boldsymbol{n}$, we can obtain that $V_{\mathrm{gq}} = -\frac{\hbar^2}{2m}(H^2 - K)$ from Eq. (15), which is consistent with the results in Refs. [11,12]. Particularly, in Refs. [24,25], researchers kept the compression direction at $\boldsymbol{n}$, considered the cases where the thickness of the curved layer is uniform and the thickness is a function of position (q^a, q^b), respectively, to obtain the thickness-corrected version of the well-known geometric potential and the effective potential relevant to the couple of the inhomogeneous confinement and the ground-state energy, respectively. Different from these cases, the general geometric potential V_{gq} are due to the deviation between the

adjacent surfaces of the layer, such as the shear dislocation, which originates from the change in the direction of compression in the confining potential method. To be specific, in the following, we will investigate the general geometric effects on the cylinder geometry based on Eqs. (14) and (15).

3. Cylindrical layers with deviations

It is well known that the cylinder geometry is a typical nanostructure, and its extensive investigation involves various nanotubes.[5,26–29] We consider a cylindrical thin-layer with radius r, as shown in Fig. 2. In the cylindrical coordinate system (θ, y, ρ), the line element is given by

$$\mathrm{d}s^2 = r^2\mathrm{d}\theta^2 + \mathrm{d}y^2 + \mathrm{d}\rho^2. \tag{16}$$

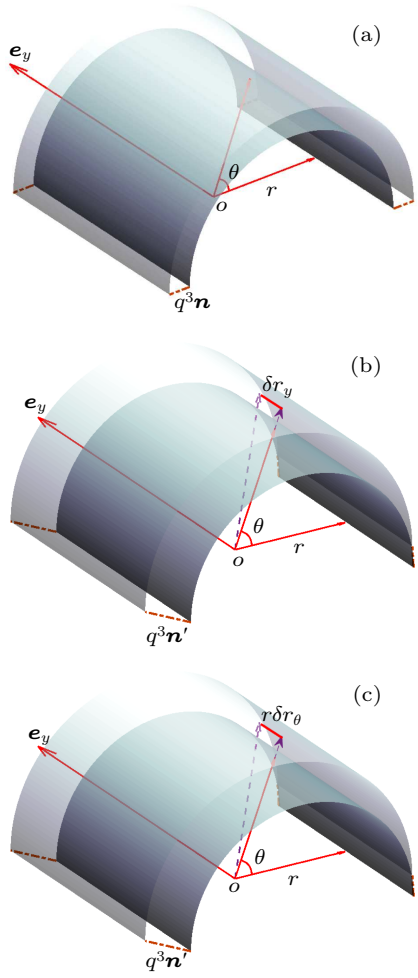


Fig. 2. Cylinder thin-layer with different deviations. (a) Normal compression, (b) slant compression, (c) tangent compression.

With the above definitions of metrics Eq. (5), the first and second fundamental forms of the cylinder are

$$\begin{aligned} &E = g_{\theta\theta} = r^2, \quad G = g_{yy} = 1, \quad F = g_{\theta y} = g_{y\theta} = 0, \\ &L = -r, \quad M = N = 0, \end{aligned} \tag{17}$$

and the metric tensor G_{ij} of the normal thin layers (as shown in Fig. 2(a)) can be defined as

$$G_{\theta\theta} = (r+q^3)^2, \quad G_{yy} = 1, \quad G_{\theta y} = G_{y\theta} = 0,$$
$$G_{\theta 3} = G_{3\theta} = G_{y3} = G_{3y} = 0, \quad G_{33} = 1. \tag{18}$$

When there is an offset from the adjacent surfaces of the cylindrical layer (as shown in Figs. 2(b) and 2(c)), in lights of Eq. (9), we can obtain

$$\begin{aligned} H^* &= \frac{1}{2r(1+r^2\delta {r_\theta}^2+\delta {r_y}^2)^{1/2}}, \\ K^* &= \frac{1}{(1+r^2\delta {r_\theta}^2+\delta {r_y}^2)}K = 0, \end{aligned} \tag{19}$$

where δr_θ and δr_y are the offsets along the $\boldsymbol{e}_\theta$ and $\boldsymbol{e}_y$, respectively. Following Eq. (14), the surface Schrödinger equation in cylindrical layer can be expressed as

$$\begin{aligned} &\mathrm{i}\hbar\frac{\partial\chi_{\mathrm{s}}(\theta,y)}{\partial t} = -\frac{\hbar^2}{2m}\frac{1}{(r+\eta)^2}\partial_\theta^2 - \frac{\hbar^2}{2m}\partial_y^2 + V_{\mathrm{gc}}, \\ &V_{\mathrm{gc}} = V_{\mathrm{gc}}^* + V_{\mathrm{gc}}^{**}, \end{aligned} \tag{20}$$

where V_{gc} is the general geometric potential that particle experiences. According to Eq. (15), the specific form can be expressed as

$$\begin{aligned} &C^* = \frac{1}{1+r^2\delta {r_\theta}^2+\delta {r_y}^2}, \quad C^{**} = \frac{2r\delta {r_\theta}^2}{(1+r^2\delta {r_\theta}^2+\delta {r_y}^2)^{3/2}}, \\ &V_{\mathrm{gc}} = V_{\mathrm{gc}}^* + V_{\mathrm{gc}}^{**}, \\ &V_{\mathrm{gc}}^* = -\frac{\hbar^2}{2m}\left[\frac{1+2r^2\delta {r_\theta}^2}{4r^2(1+r^2\delta {r_\theta}^2+\delta {r_y}^2)}\right], \\ &V_{\mathrm{gc}}^{**} = -\frac{\hbar^2}{2m}\left[\frac{3\delta {r_\theta}^2}{2} - \frac{\delta {r_y}^2}{2} + \frac{3\delta {r_\theta}^4 r^2}{4(1+r^2\delta {r_\theta}^2+\delta {r_y}^2)}\right]. \end{aligned} \tag{21}$$

It is straightforward to find that in the absence of the deviation ($\delta r_\theta = \delta r_y = 0$), $V_{\mathrm{gc}} = -\frac{\hbar^2}{2m}\frac{1}{4r^2}$ agrees with the previous results in Refs. [16,30]. To elaborately analyze the geometric effects resulting from deviations, in the following, we will take two cases into consideration.

(i) $\delta r_\theta = 0$, $\delta r_y \neq 0$. The compression form should turn from normal compression to slant compression, as shown in Fig. 2(b). And equation (21) is expressed as

$$\begin{aligned} &C_y^* = \frac{1}{1+\delta {r_y}^2}, \quad C_y^{**} = 0, \\ &V_{\mathrm{gcy}} = V_{\mathrm{gcy}}^* + V_{\mathrm{gcy}}^{**}, \\ &V_{\mathrm{gcy}}^* = -\frac{\hbar^2}{2m}\left[\frac{1}{4r^2(1+\delta {r_y}^2)}\right], \\ &V_{\mathrm{gcy}}^{**} = -\frac{\hbar^2}{2m}\left[-\frac{\delta {r_y}^2}{2}\right]. \end{aligned} \tag{22}$$

The specific properties of V_{gcy}^*, V_{gcy}^{**}, and V_{gcy} versus $\tan\beta = \delta r_y/r$ are described in Fig. 3. Clearly, V_{gcy}^* is always negative, and the larger deviation raises up it. Besides, for a thicker layer with a larger radius r, the effect of V_{gcy}^* would become weaker. Compared to the potential V_{gcy}^*, the deviation-dependent term V_{gcy}^{**} acts as a parabolic-barrier. The differences between the potentials V_{gcy}^{**} and V_{gcy}^* are their signs, which can compensate for or even overwrite the value of V_{gcy}^*,

and this kind of effect is enhanced for the larger offset and smaller curvature radius. Together with these potentials, in the case of small radius accompanied with negligible deviation, $V_{\rm gcy}$ may result in the appearance of the bound states,[7,8,31,32] while as the deviation increases, the bound states will disappear and $V_{\rm gcy}$ would shift the spectrum in different directions.

(ii) $\delta r_y = 0, \delta r_\theta \neq 0$. At this time, the tangent compression is employed, as shown in Fig. 2(c). Here the general geometric potential Eq. (15) takes the form as

$$
\begin{aligned}
C_\theta^* &= \frac{1}{1+r^2\delta {r_\theta}^2}, \quad C_\theta^{**} = \frac{2r\delta {r_\theta}^2}{(1+r^2\delta {r_\theta}^2)^{3/2}},\\
V_{{\rm gc}\theta} &= V_{{\rm gc}\theta}^* + V_{{\rm gc}\theta}^{**},\\
V_{{\rm gc}\theta}^* &= -\frac{\hbar^2}{2m}\left[\frac{1+2r^2\delta {r_\theta}^2}{4r^2(1+r^2\delta {r_\theta}^2)}\right]\\
&= -\frac{\hbar^2}{2m}\left[\frac{1+2(r\delta r_\theta)^2}{4r^2(1+(r\delta r_\theta)^2)}\right],
\end{aligned}
$$

$$
\begin{aligned}
V_{{\rm gc}\theta}^{**} &= -\frac{\hbar^2}{2m}\left[\frac{3\delta {r_\theta}^2}{2} + \frac{3\delta {r_\theta}^4 r^2}{4(1+r^2\delta {r_\theta}^2)}\right]\\
&= -\frac{\hbar^2}{2m}\left[\frac{3(r\delta r_\theta)^2}{2r^2} + \frac{3(r\delta r_\theta)^4}{4r^2(1+(r\delta r_\theta)^2)}\right]. \qquad (23)
\end{aligned}
$$

Figure 4 describes $V_{{\rm gc}\theta}^*$, $V_{{\rm gc}\theta}^{**}$, and $V_{{\rm gc}\theta}$ versus $\tan\gamma = r\delta r_\theta/r$ for the cases of $r = 0.25$, $r = 0.5$, and $r = 1$. It is obvious to find that both $V_{{\rm gc}\theta}^*$ and $V_{{\rm gc}\theta}^{**}$ are all negative. Compared with the two, the deviation term $V_{{\rm gc}\theta}^{**}$ plays a main role, manifests as significantly suppressing the effective potential and generally drops as the deviation increases, which is differ from the case of slant compression. Therefore, the combined potential $V_{{\rm gc}\theta}$ shows the similar trend as those for $V_{{\rm gc}\theta}^{**}$. Considering for instance a value of $r = 0.5$ and $\tan\gamma = 5$, $V_{{\rm gc}\theta} = -13.843$, compared to $V_{\rm gc} = -1$, we find an enhancement of typical geometric potential by over 10, the geometric potential wells are dramatically deepened, especially in the smaller radius and larger deviation, which naturally generates new bound states. These results are helpful to change the band structure and manipulate the electron transport.[28,29]

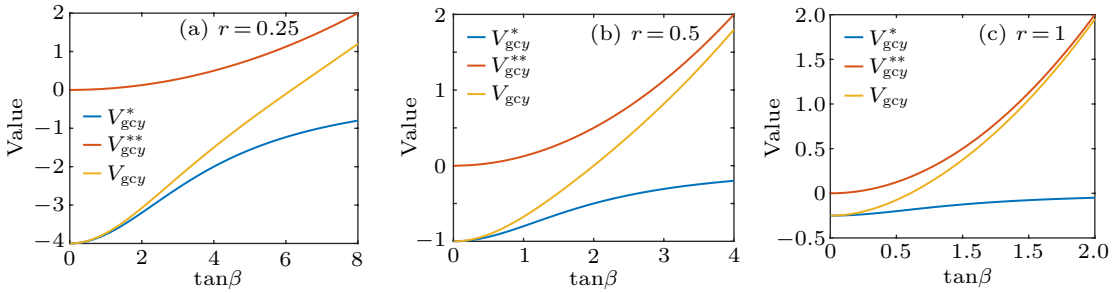


Fig. 3. The $V_{\rm gcy}^*$, $V_{\rm gcy}^{**}$, and $V_{\rm gcy}$ versus $\tan\beta = \delta r_y/r$ for the cases of $r = 0.25, 0.5, 1$. Here, $\hbar^2/2m^*$ is taken as a unit.

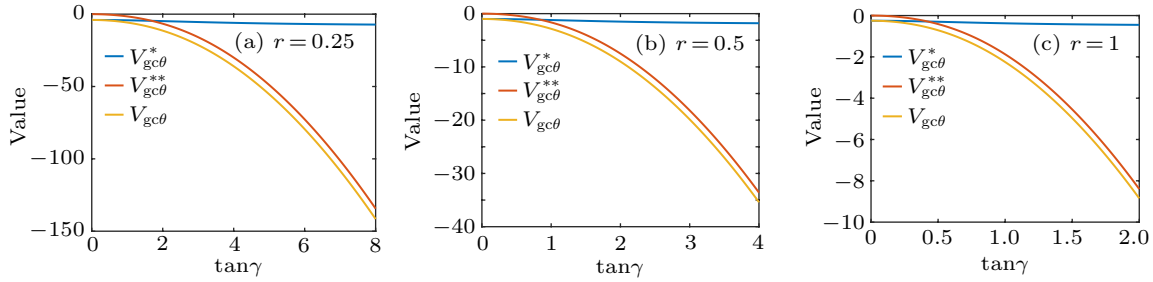


Fig. 4. The $V_{{\rm gc}\theta}^*$, $V_{{\rm gc}\theta}^{**}$, and $V_{{\rm gc}\theta}$ versus $\tan\gamma = r\delta r_\theta/r$ for the cases of $r = 0.25, 0.5, 1$. Here, $\hbar^2/2m^*$ is taken as a unit.

4. Discussion and conclusion

In conclusion, we have considered quantum physics related to a curved thin-layer with the deviation. Using the confining potential method in the treatment of general compression form, we derived the surface Schrödinger equation with a general geometric potential, which is taken as an equivalent description of the quantum dynamics within curved layers. The deviation renders a gigantic renormalization of the quantum geometric potential which has very significant consequences for the electronic properties of the nano-materials. Applying our theoretical framework to the case of cylindrical thin layer, we find two types of the general geometric potential $V_{\rm gcy}$ and $V_{{\rm gc}\theta}$, which corresponds to the slant compression and tangent compression, respectively. The former weakens the constrain on the bounded particles, making them behave like free-particles. While the latter significantly strengthen the constrain, which accumulates the negative level eigenstates in the low-energy part of the electronic energy spectrum. What is more, the combined potential $V_{\rm gc}$ is still valid to arbitrary deviation regarded as a combination of the slant deviation and tangent deviation. These potentials can effectively manipulate the band-structure bases on theirs ability to change the role played by potentials.

In addition to the geometric potential, the geometric effect can also be shown by geometric momentum (GM) whose operator is $\boldsymbol{P} = -\mathrm{i}\hbar\nabla_{\Sigma} + H\boldsymbol{n}$,[14,15,33] where ∇_{Σ} denotes the gradient operator acted on the surface and $H\boldsymbol{n}$ symbolizes the mean curvature vector field. Based on the result V_{gq}, the introduce of the deviation $\delta\boldsymbol{r}$ should allow a new field $H^{*}\boldsymbol{n}'$ replaces $H\boldsymbol{n}$ in the case of curved layer. Can the corrected GM operator be taken as the generators of the infinitesimal parallel transport of a vector on the curved thin layer with the deviation, which is still an interesting project that needs further investigation.

As a potential application, the deviations between the adjacent surfaces of the thin layer can be employed not only to guide the shift direction of the energy level structures, but also to manipulate the transport properties of nano-materials based on the bound states they generate. These results provide a prospect of possible application to design soft nano-based devices by adjusting the offsets between the substrate and attachment.

Acknowledgements

Project jointly supported by the National Natural Science Foundation of China (Grant No. 11934008). Cheng R was funded by the Fund from National Laboratory of Solid State Microstructure of Nanjing University (Grant Nos. M35040 and M35053) and the Youth Independent Innovation Fund (Grant No. KYJBJKQTZQ23006).

References

[1] Takahata K 2014 *Advances in micro/nano electromechanical systems and fabrication technologies*
[2] Prinz V Y, Seleznev V A, Gutakovsky A K, Chehovskiy A V, Preobrazhenskii V V, Putyato M A and Gavrilova T A 2000 *Physica E* **6** 828
[3] Ozaki T, Iwasa Y and Mitani T 2000 *Phys. Rev. Lett.* **84** 1712
[4] Schmidt O G and Eberl K 2001 *Nature* **410** 168
[5] Ortix C and van den Brink J 2010 *Phys. Rev. B* **81** 165419
[6] Ortix C and van den Brink J 2011 *Phys. Rev. B* **83** 113406
[7] Cheng R, Wang Y L, Gao H X, Zhao H, Wang J Q and Zong H S 2020 *J. Phys.: Condes. Matter* **32** 025504
[8] Cheng R, Wang Y L, Zhao H, Ye C Z, Liang G H and Zong H S 2021 *Results Phys.* **22** 103974
[9] Pereira L F C, Andrade F M, Filgueiras C and Silva E O 2021 *Physica E* **132** 114760
[10] Pereira L F C, Andrade F M, Filgueiras C and Silva E O 2022 *Few-Body Syst.* **63** 64
[11] Jensen H and Koppe H 1971 *Ann. Phys.* **63** 586
[12] da Costa R C T 1981 *Phys. Rev. A* **23** 1982
[13] Schuster P and Jaffe R 2003 *Ann. Phys.* **307** 132
[14] Liu Q H, Tong C L and M L M 2007 *J. Phys. A: Math. Theor.* **40** 4161
[15] Liu Q H, Tang L H and Xun D M 2011 *Phys. Rev. A* **84** 042101
[16] Cheng R, Wang L, Zhao H, Luo C B, Wang Y L and Wang J 2021 *Commun. Theor. Phys.* **73** 125004
[17] Cheng R, Wang L, Zhao H, Wang Y L and Wang J 2022 *Results Phys.* **42** 105974
[18] Wang Y L, Du L, Xu C T, Liu X J and Zong H S 2014 *Phys. Rev. A* **90** 042117
[19] Szameit A, Dreisow F, Heinrich M, Keil R, Nolte S, Tünnermann A and Longhi S 2010 *Phys. Rev. Lett.* **104** 150403
[20] Songmuang R, Deneke C and Schmidt O 2006 *Appl. Phys. Lett.* **89** 223109
[21] Liang S, Zhang M, Biesold G M, Choi W, He Y, Li Z, Shen D and Lin Z 2021 *Adv. Mater.* **33** 2005888
[22] Zhang F, Yang K, Liu G, Chen Y, Wang M, Li S and Li R 2022 *Compos Part A: Appl. Sci. Manuf.* **160** 107051
[23] Shikakhwa M and Chair N 2022 *Eur. Phys. J. Plus* **137** 560
[24] Wang Y L and Zong H S 2016 *Ann. Phys.* **364** 68
[25] Liang G H and Lai M Y 2023 *Phys. Rev. A* **107** 022213
[26] Goldstone J and Jaffe R L 1992 *Phys. Rev. B* **45** 14100
[27] Ouyang P, Mohta V and Jaffe R 1999 *Ann. Phys.* **275** 297
[28] Santos F, Fumeron S, Berche B and Moraes F 2016 *Nanotechnology* **27** 135302
[29] Cheng R, Wang Y L, Jiang H, Liu X J and Zong H S 2019 *Condens. Matter* **4** 3
[30] Ferrari G and Cuoghi G 2008 *Phys. Rev. Lett.* **100** 230403
[31] Encinosa M and Etemadi B 1998 *Phys. Rev. A* **58** 77
[32] Encinosa M and Mott L 2003 *Phys. Rev. A* **68** 014102
[33] Spittel R, Uebel P, Bartelt H and Schmidt M A 2015 *Opt. Express* **23** 12174